Proceedings of ENCIT 2010
Copyright © 2010 by ABCM
13rd Brazilian Congress of Thermal Sciences and Engineering
December 05-10, 2010, Uberlandia, MG, Brazil

SYNCHRONIZATION OF VORTEX FORMATION FREQUENCY WITH THE BODY MOTION FREQUENCY AT HIGH REYNOLDS NUMBER

Luiz Antonio Alcântara Pereira, luizantp@unifei.edu.br
Institute of Mechanical Engineering, Federal University of Itajubá, CP 50, Av. BPS 1303, CEP. 37500-903, Itajubá, Minas Gerais, Brazil.

Miguel Hiroo Hirata, hirata@fat.uerj.br
State University of Rio de Janeiro, FAT-UERJ, Resende, Rio de Janeiro, Brazil.

***Abstract**. Understanding vortex induced vibrations is of great importance in the design of a variety of offshore engineering structures, nuclear plant components and cylindrical elements in tube-bank heat exchangers, for example. If a body is placed in a flow, it experiences alternating lift and drag forces caused by the asymmetric formation of vortices, which can cause a structure to vibrate. One of the most interesting features of this flow is the phenomenon of lock-in which is observed when the vortex shedding frequency is close to the body oscillation frequency. This paper presents the results of numerical experiments on vortex shedding from a circular cylinder vibrating in-line or transversely with an incident uniform flow at Reynolds number of 1.0×10^5. The frequencies of the lift and drag coefficients are compared with the body motion frequency when the frequency ratio is about unity.*

***Keywords**: Vortex method, Bluff body, Aerodynamic loads, Forced oscillations, Lock-in.*

1. INTRODUCTION

The flow around circular cylinder includes a variety of fluid dynamics phenomena, such as separation from a body surface, vortex shedding and the formation of a large wake. Results reported in the literature showed that vortex shedding could be dramatically changed when a cylinder is oscillating in a fluid stream (Williamson and Roshko, 1988). One of the most interesting features of this flow is the phenomenon of synchronization, in which the frequency of vortex shedding, f, coincides with that of the cylinder oscillation, f_b; this is also known as "lock-in".

Previous works have reported that the lock-in features and vortex shedding patterns in the flow around an in-line oscillating cylinder differ significantly with those in flows around a stationary cylinder or a cylinder oscillating transversely. For instance, vortex shedding frequency f had been found to lock-in to the forcing frequency f_{by} when f_{by} is close to the free vortex shedding frequency f_{so} in the transverse oscillating case. But, the in-line vibration lock-in takes place at a number of multiple ratios of f_{bx}/f_{so}, especially, at $f_{bx}/f_{so}=2.0$, where the lift and drag forces increase greatly. Comprehensive reviews can be found in Koopman (1967), Sarpkaya (1979), Bearman (1984), Blevins (1990), Griffin and Hall (1991), Williamson and Govardhan (2004) and Hirata *et al.* (2008).

Koopman (1967) investigated the lock-in region in terms of the oscillation amplitude A_x and the frequency of a circular cylinder f_{bx}. He showed that the Kármán vortex is more likely to lock-in when f_{bx} is closer to the vortex shedding frequency from the fixed cylinder, f_{s0}, i.e. the threshold amplitude is lower when f_{bx}/f_{s0} is closer to unity. He also reported that there exists a definite value of oscillation amplitude below which the lock-in does not occurs even when $f_{bx}/f_{s0}=1.0$.

The experimental work of Williamson and Roshko (1988) deals with the synchronization regions and identifies many modes and vortex wake patterns with detailed explanations and descriptions; due to the difficulties in the experimental visualizations the Reynolds number were kept below 600.

Ongoren and Rockwell (1988) carried out extensive experiments from an in-line oscillating circular cylinder at low Reynolds number Re=855. Two basic vortex shedding patterns were observed for the forced oscillation for $A_x/d=0.13$ (d is the diameter cylinder): one with symmetrical mode and the other with four antisymmetrical modes. According their experiments, in general, the cylinder oscillations are predominantly in the symmetrical mode, while the antisymmetrical modes are induced by the naturally occurring large-scale vortex formation.

The numerical work of Hirata *et al.* (2008) simulated the flow around a heaving circular cylinder by using vortex method. Their results showed that there are three characteristic bands for the body oscillating frequency. Band I, for which $f_b \rightarrow 0$, the body oscillation has little influence and the vortex shedding frequency is almost independent of the body oscillating frequency. Band II represents a transition band in which the lock-in is partial and one can identify simulation periods in which lock-in is observed followed by simulation periods where this does not occurs. Finally in the uppermost Band III the inertial components dominate the lock-in is always observed, as will be reported latter in Fig. 2. The numerical findings show that the lock-in frequency depends on the amplitude of the body oscillation; in fact it decreases linearly with it in accordance of the low Reynolds number findings of Williamson and Roshko (1988).

The present paper utilizes the vortex method code developed by Hirata *et al.* (2008) to simulate numerically the vortex shedding from an in-line or transversal oscillating circular cylinder in a uniform flow at high Reynolds number of 1.0×10^5. In this study, the frequencies of the lift and drag coefficients are compared with the body motion frequency when the frequency ratio is about unity. The transition behavior from non lock-in to lock-in is investigated by using two reference frames; the body fixed frame oscillates with respect to the inertial frame of reference. A cloud of free vortices is used in order to simulate the vorticity, which is generated on the body surface and develops into the boundary layer and the viscous wake. Each individual free vortex of the cloud is followed during the numerical simulation in a typical Lagrangian scheme. Important features of the vortex method (Chorin, 1973; Leonard, 1980; Sarpkaya, 1989; Lewis, 1999; Alcântara Pereira *et al.*, 2004; Stock, 2007; Kamemoto, 2009) are: (i) it is a numerical technique suitable for the solution of convection/diffusion type equations like the Navier-Stokes ones; (ii) it is a suitable technique for direct simulation and large-eddy simulation; (iii) it is a mesh free technique; the vorticity field is represented by a cloud of discrete free vortices that move with the fluid velocity.

Vortex cloud simulation offers a number of advantages over the more traditional Eulerian schemes for the analysis of the external flow that develops in a large domain; the main reasons are: (i) as a fully mesh-less scheme, no grid is necessary; (ii) the computational efforts are directed only to the regions with non-zero vorticity and not to all the domain points as is done in the Eulerian formulations; (iii) the far away downstream boundary condition is taken care automatically which is relevant for the simulation of the flow around a bluff body (or an oscillating body) that has a wide viscous wake and (iv) moving or deforming boundary problems are easily dealt with.

The two-dimensional aerodynamic characteristics are investigated at a higher Reynolds number; due to this fact, even with such a high Reynolds number value, no attempt for turbulence modeling were made once these aspects have a strong three-dimensional component; see Alcântara Pereira *et al.* (2002).

2. FORMULATION OF THE PROBLEM

2.1. Definitions

Figure 1 shows the in-line and transversal motions of a point P located at the circular cylinder surface and viewed from the (x, o, y), which is defined as the inertial frame of reference. A second frame of reference (ξ, o, η) is defined as the coordinate system fixed to the cylinder and, therefore, free to oscillates in a harmonic motion.

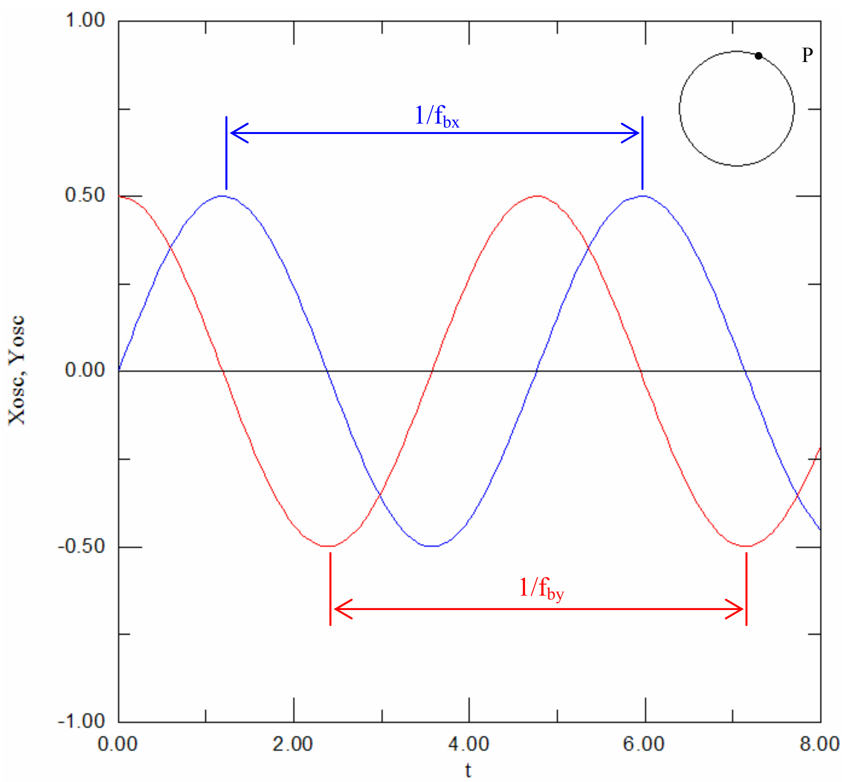

Figure 1 – Sketch of in-line and transversal oscillating cylinder.

The position and velocity of the local moving coordinate at the center of the circular cylinder are defined, respectively, as

$$\xi_x = A_x \sin(\lambda_x\ t) \text{ and } \eta_y = A_y \cos(\lambda_y\ t), \tag{1}$$

$$\dot{\xi}_x = u_{oscx} = A_x\ \lambda_x \cos(\lambda_x\ t) \text{ and } \dot{\eta}_y = v_{oscy} = -A_y\ \lambda_y \sin(\lambda_y\ t). \tag{2}$$

where A_x and A_Y are the body oscillation amplitudes, $\lambda_x=2\pi f_{bx}$ and $\lambda_y=2\pi f_{by}$ are the angular velocities, f_{bx} and f_{by} are the body oscillation frequencies and t is the time in the physical domain.

The boundary S of the fluid domain can be defined as $S = S_b \cup S_\infty$; being S_b the circular cylinder surface (which contains the P point) and S_∞ the far away boundary (which can be viewed as $r = \sqrt{x^2 + y^2} \to \infty$).

2.2. Governing Equations

For an incompressible fluid flow the continuity is written as

$$\nabla \cdot \mathbf{u} = 0 \tag{3}$$

where $\mathbf{u} \equiv (u, v)$ is the velocity vector.

If, in addition, the fluid is Newtonian with constant properties the momentum equation is represented by the Navier-Stokes equation as

$$\frac{\partial \mathbf{u}}{\partial t} + \mathbf{u} \cdot \nabla \mathbf{u} = -\nabla p + \frac{1}{Re} \nabla^2 \mathbf{u}\ . \tag{4}$$

Here, p is the pressure field and Re stands for the Reynolds number defined as $Re = \frac{U\,d}{\upsilon}$, where υ the kinematic viscosity of fluid and d is the diameter cylinder; the dimensionless time is d/U.

On the cylinder surface the adherence condition has to be satisfied. This condition is better specified in terms of the normal and tangential components as

$$(\mathbf{u} \cdot \mathbf{n}) = (\mathbf{v} \cdot \mathbf{n}) \text{ on } S_b \text{, the impenetrability condition} \tag{5}$$

$$(\mathbf{u} \cdot \boldsymbol{\tau}) = (\mathbf{v} \cdot \boldsymbol{\tau}) \text{ on } S_b \text{, the no-slip condition} \tag{6}$$

where $\mathbf{n}$ and $\boldsymbol{\tau}$ are unit normal and tangential vectors and $\mathbf{v}$ is the body surface velocity vector.

Far from the body (for $r\to\infty$, in Fig. 1) one assumes that the perturbation due to the body motion fades away, that is

$$|\mathbf{u}| \to 1\ . \tag{7}$$

3. THE VORTEX METHOD

3.1. Viscous Splitting Algorithm (Chorin, 1973)

Taking the curl of the Navier-Stokes equation and with some algebraic manipulations one gets the vorticity equation which presents no pressure term. In two-dimensions this equation reads

$$\frac{\partial \omega}{\partial t} + \mathbf{u} \cdot \nabla \omega = \frac{1}{Re} \nabla^2 \omega \tag{8}$$

where $\omega(\mathbf{x}, t) = \nabla \times \mathbf{u}(\mathbf{x}, t)$ represents the only non-zero component of the vorticity field (observe that the pressure is absent from the formulation).

The left hand side of the above equation carries all the information needed for the convection of vorticity while the right hand side governs the diffusion. Following Chorin (1973) we use the viscous splitting algorithm, which, for the same time step of the numerical simulation, says that

Convection of vorticity is governed by

$$\frac{\partial \omega}{\partial t} + \mathbf{u} \cdot \nabla \omega = 0 \tag{9}$$

Diffusion of vorticity is governed by

$$\frac{\partial \omega}{\partial t} = \frac{1}{Re} \nabla^2 \omega . \tag{10}$$

3.2. Convection and diffusion of vorticity

The vortex method proceeds by discretizing spatially the vorticity field using a cloud of elemental vortices, which are characterized by a distribution of vorticity, ς_{σ_i} (commonly called the cutoff function), the circulation strength Γ_i and the core size σ_i. Thus, the discretized vorticity is expressed by

$$\omega(\mathbf{x}, t) \approx \omega^h(\mathbf{x}, t) = \sum_{i=1}^{Z} \Gamma_i(t) \varsigma_{\sigma_i}(\mathbf{x} - \mathbf{x}_i(t)) . \tag{11}$$

where Z is the number of point vortices of the cloud used to simulate the vorticity field.

In this paper, as the diffusion effects are simulated using the random displacement method (Lewis, 1999), we assume that the core sizes are uniform ($\sigma_i = \sigma$), and use the Gaussian distribution as the cut-off function; this choice of the cut-off function leads to the Lamb Vortices (Leonard, 1980); thus

$$\varsigma_\sigma(\mathbf{x}) = \frac{1}{\pi\sigma^2} \exp\left(-\frac{|\mathbf{x}|^2}{\sigma^2} \right) . \tag{12}$$

The numerical analysis is conducted over a series of small discrete time steps Δt for each of which a discrete vortex element $\Gamma_{(i)}$ is shed from each impeller surface element. The intensity $\Gamma_{(i)}$ of these newly generated vortices is determined using the no-slip condition, see Eq. (6).

For the convection of the discrete vortices of the cloud, Eq. (9) is written in its Lagrangian form as

$$\frac{dx^{(i)}}{dt} = u^{(i)}(x, y, t) \tag{13}$$

$$\frac{dy^{(i)}}{dt} = v^{(i)}(x, y, t) \tag{14}$$

being (i) = 1, Z.

The convective motion of each vortex generated on the body surface is determined by integration of each vortex path equation, which can be written, using a first order Euler scheme, as

$$x^{(i)}(t + \Delta t) = x^{(i)}(t) + \left[u^{(i)}(t) \right] \Delta t \tag{15}$$

$$y^{(i)}(t + \Delta t) = y^{(i)}(t) + \left[v^{(i)}(t) \right] \Delta t . \tag{16}$$

The diffusion of vorticity is taken care of using the random walk method (Lewis, 1999). The random displacement $Z_d \equiv (x_d, y_d)$, with a zero mean and a $(2\Delta t/Re)$ variance, for vortex (i) is defined as

$$x_d^{(i)} = [\cos(2\pi Q)] \sqrt{\frac{4\Delta t}{Re} \ln\left(\frac{1}{P}\right)} \tag{17}$$

$$y_d^{(i)} = [\sin(2\pi Q)] \sqrt{\frac{4\Delta t}{Re} \ln\left(\frac{1}{P}\right)} \tag{18}$$

where P and Q are random numbers in the range 0.0 to 1.0. Therefore the final displacement is written as

$$x^{(i)}(t+\Delta t) = x^{(i)}(t) + \left[u^{(i)}(t)\right]\Delta t + x_d^{(i)} \tag{19}$$

$$y^{(i)}(t+\Delta t) = y^{(i)}(t) + \left[v^{(i)}(t)\right]\Delta t + y_d^{(i)}\,. \tag{20}$$

3.3. Numerical Implementation

The $u^{(i)}$ and $v^{(i)}$ components of the velocity induced at the location of the vortex (i) can be written as

$$u^{(i)} = 1 + ub^{(i)} + uv^{(i)} \tag{21}$$

$$v^{(i)} = 0 + vb^{(i)} + vv^{(i)} \tag{22}$$

where, $\mathbf{ui}^{(i)} \equiv [1, 0]$ is the velocity vector of uniform flow,

$\mathbf{ub}^{(i)} \equiv [ub^{(i)}, vb^{(i)}]$ is the velocity vector induced by the cylinder at the location of vortex (i),

$\mathbf{uv}^{(i)} \equiv [uv^{(i)}, vv^{(i)}]$ is the velocity vector induced at the vortex (i) due to the vortex cloud.

The $\mathbf{ui}^{(i)}$ calculations present no problems. The body contributes with $\mathbf{ub}(\mathbf{x}, t)$, which can be obtained, for example, using the Boundary Element Method (Katz and Plotkin, 1991). The two components can be written as

$$ub^{(i)} = \sum_{k=1}^{NP} \psi_k\, uc_k^{(i)} \tag{23}$$

$$vb^{(i)} = \sum_{k=1}^{NP} \psi_k\, vc_k^{(i)} \tag{24}$$

where NP is the total number of flat source panels representing cylinder surface. It is assumed that the source strength per length is constant such that ψ_k = const and $uc_k^{(i)}$ and $vc_k^{(i)}$ are the components of the velocity induced at vortex (i) by a unit strength flat source panel located at k.

As the body surface is simulated by NP straight line panels (Panels Method) it is convenient to calculate the body induced velocity in the moving coordinate system. For that one has to observe the following

- The fluid velocity on the body surface is written as

$$\mathbf{u}(\xi, \eta; t) = \left\lfloor A_x\,\lambda_x \cos(\lambda_x\, t)\right\rfloor \mathbf{i} + \left\lfloor -A_y\,\lambda_y \sin(\lambda_y\, t)\right\rfloor \mathbf{j}\,. \tag{25}$$

- The velocity induced by the body, according to the Panels Method calculations, is indicated by [ub(ξ,η), vb(ξ,η)]; this is the velocity induced at the vortex (i), located at the point [ξ(t), η(t)]; thus

$$ub^{(i)}(x, y; t) = ub(\xi, \eta; t) + A_x\,\lambda_x \cos\left(\lambda_x\, t\right) \tag{26}$$

$$vb^{(i)}(x, y; t) = vb(\xi, \eta; t) - A_y\,\lambda_y \sin\left(\lambda_y\, t\right). \tag{27}$$

The velocity $\mathbf{uv}$ is obtained from the vorticity field by means of the Biot-Savart law

$$\mathbf{uv}(\mathbf{x}, t) = \int (\nabla \times \mathbf{G})(\mathbf{x} - \mathbf{x}')\omega(\mathbf{x}', t)d\mathbf{x}' = \int \mathbf{K}(\mathbf{x} - \mathbf{x}')\omega(\mathbf{x}', t)d\mathbf{x}' = (\mathbf{K} * \omega)(\mathbf{x}, t) \tag{28}$$

where $\mathbf{K} = \nabla\times\mathbf{G}$ is the Biot-Savart kernel, $\mathbf{G}$ is the Green's function for the Poisson equation, and $*$ represents the convolution operation.

Once, with the vorticity field the pressure calculation starts with the Bernoulli function, defined by Uhlman (1992) as

$$\overline{Y} = p + \frac{u^2}{2}, \ u = |\mathbf{u}| . \tag{29}$$

Kamemoto (1993) used the same function and starting from the Navier-Stokes equations was able to write a Poisson equation for the pressure. This equation was solved using a finite difference scheme. Here the same Poisson equation was derived and its solution was obtained through the following integral formulation (Shintani and Akamatsu, 1994)

$$H\overline{Y_i} - \int_S \overline{Y}\nabla\Xi_i \cdot \mathbf{e}_n dS = \iint_\Omega \nabla\Xi_i \cdot (\mathbf{u}\times\boldsymbol{\omega}) d\Omega - \frac{1}{Re}\int_S (\nabla\Xi_i \times \boldsymbol{\omega}) \cdot \mathbf{e}_n dS \tag{30}$$

where $H = 1$ in the fluid domain, $H = 0.5$ on the boundaries, Ξ is a fundamental solution of the Laplace equation and $\mathbf{e}_n$ is the unit vector normal to the solid surfaces.

The drag and lift coefficients are expressed by (Ricci, 2002)

$$C_D = -\sum_{k=1}^{NP} 2(p_k - p_\infty)\Delta S_k \sin\beta_k = -\sum_{k=1}^{NP} C_P \Delta S_k \sin\beta_k \tag{31}$$

$$C_L = -\sum_{k=1}^{NP} 2(p_k - p_\infty)\Delta S_k \cos\beta_k = -\sum_{k=1}^{NP} C_P \Delta S_k \cos\beta_k \tag{32}$$

where ΔS_k is the length and β_k is the angle and both of the k^{th}-panel.

4. RESULTS AND DISCUSSION

The flow around a stationary circular cylinder in a uniform flow at Reynolds number of 1.0×10^5 is investigated to analyze the consistence of the vortex code and to define some numerical parameters; as for example the number of panels used to define the cylinder surface. Based on the numerical results, the cylinder surface was represented by NP=100 flat source panels with constant density. The simulation was performed up to 800 time steps with magnitude $\Delta t=0.05$. During each time step the new vortex elements are shedding into the cloud through a displacement $\varepsilon=\sigma_0=0.0032d$ normal to the straight-line elements (panels); see Ricci (2002).

Drag and lift coefficients are investigated to compute the vortex shedding frequency and to define the harmonic motion of the cylinder. Table 1 shows that the numerical results agree very well with the experimental ones obtained by Blevins (1984), which have an uncertainty of about 10%. The present drag coefficient shows a higher value as compared to the experimental result. One should observe that the three-dimensional effects are non-negligible for the Reynolds number used in the present simulation. Therefore one can expect that a two-dimensional computation of such a flow must produce higher values for the drag coefficient. On the other hand, the Strouhal number is insensitive to these three-dimensional effects. The mean numerical lift coefficient, although very small, is not zero which is due to numerical approximations. The aerodynamic forces computations were evaluated between t=20 and t=40.

Table 1. Mean drag and lift coefficients and Strouhal number for stationary circular cylinder

$Re = 1.0\times10^5$	$\overline{C_D}$	$\overline{C_L}$	$\overline{St} = f_{s0}$
Blevins (1984)	1.20	-	0.19
Present Simulation	1.22	0.07	0.20

The Strouhal number is defined as

$$St = \frac{f\,d}{U} \tag{33}$$

where f is the detachment frequency of vortices of the lift coefficient. According results, when vortices are shed into the wake of a stationary circular cylinder, they cause a periodic lift force on the body at a frequency of shedding, $1.0f_{s0}$, and a drag force having twice that frequency, $2.0f_{s0}$. More details of this preliminary study are discussed in Hirata *et al.* (2008).

In this paper, the body Strouhal number is defined as

$$St_c = \frac{f_b d}{U} . \tag{34}$$

Figure 2 shows typical results of the flow around a heaving cylinder at Reynolds number of 1.0×10^5 with small and large amplitudes, in which the abscissa is the body Strouhal number St_c and the ordinate is the Strouhal number for stationary cylinder, see Eq. (33). The numerical simulations show that the flow is influenced mainly by the body oscillation amplitude A_y and the body motion frequency $f_{by.}$

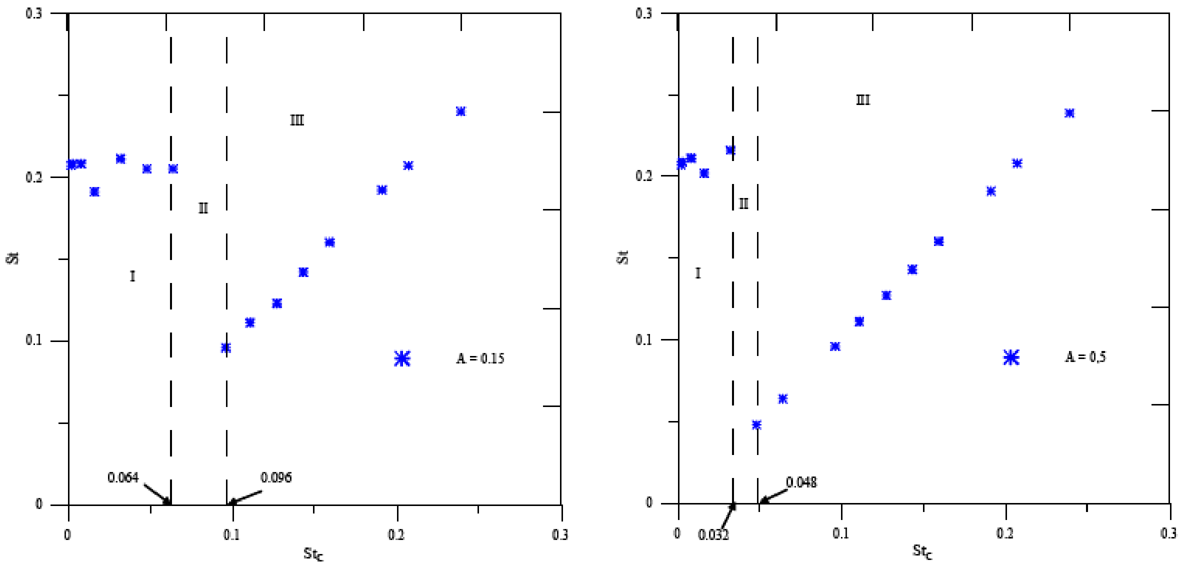

(a) A_y/d=0.15 (b) A_y/d=0.50

Figure 2 – Oscillation of cylinder transverse to the flow: Synchronization at Band III of the vortex shedding frequency (St) with the body motion frequency (St_c) for oscillation amplitudes A_y/d=0.15 and A_y/d=0.50.

Hirata *et al.* (2008) showed that in general the high Reynolds number simulations agree quite well the low Reynolds number vortex synchronization regions described by Williamson and Roshko (1988).

The present numerical results permit concludes that when the oscillating frequency of the cylinder is at or near the frequency of vortex shedding from a stationary cylinder, the vortex shedding synchronizes with the cylinder motion. Figure 3 illustrates the vortex cloud structure for a transversely oscillating cylinder when occurs the synchronization of the vortex shedding frequency (St) with the body motion frequency (St_c) for large amplitude.

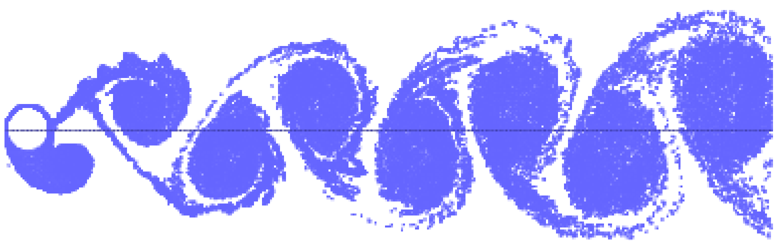

Figure 3 – Vortex cloud structure for transversely oscillating cylinder (A_y/d=0.50 and f_{by}/f =1.0).

Figure 4 shows the variation of the drag and lift coefficients with time for in-line oscillating circular cylinder in the uniform flow. Two regimes of vortex shedding are identified.

First, in the Fig. 4a, case when $A_x/d=0.13$ and $f_{bx}/f_{cd}=1.0$ (being f_{cd} the frequency of the drag coefficient), the lift curve has the same frequency as the drag coefficient and has a single local peak during a cycle. This mode of vortex shedding, defined as mode AI, was observed by Ongoren and Rockwell (1988). The numerical work by Liu and Song (2003) presented several types of vortex shedding mode, including mode AI. In their work the Reynolds number was Re=855.

Second, in the Fig. 4b, case when $A_x/d=0.50$ and $f_{bx}/f_{cd}=1.0$, the lift coefficient no oscillates and the frequency of oscillation of the drag coefficient curve is closer to the vortex shedding frequency from the fixed cylinder. This mode of vortex shedding is defined as symmetrical mode S.

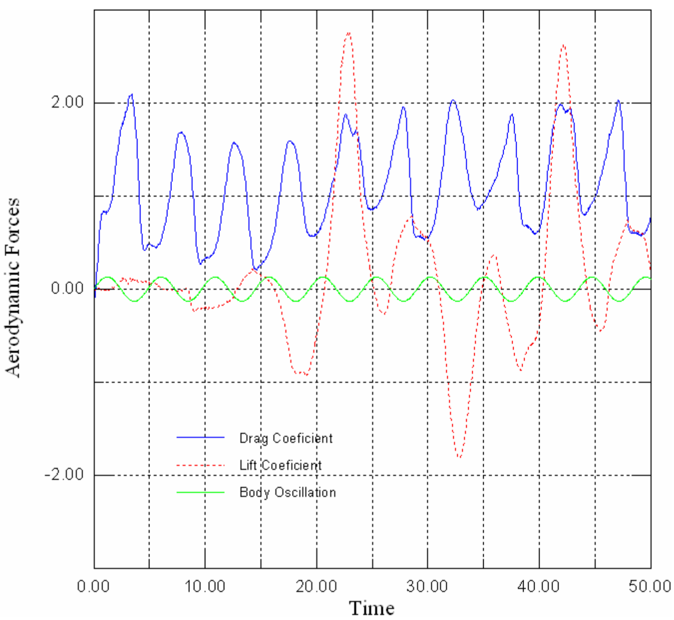

(a) $A_x/d=0.13$ and $f_{bx}/f_{cd}=1.0$

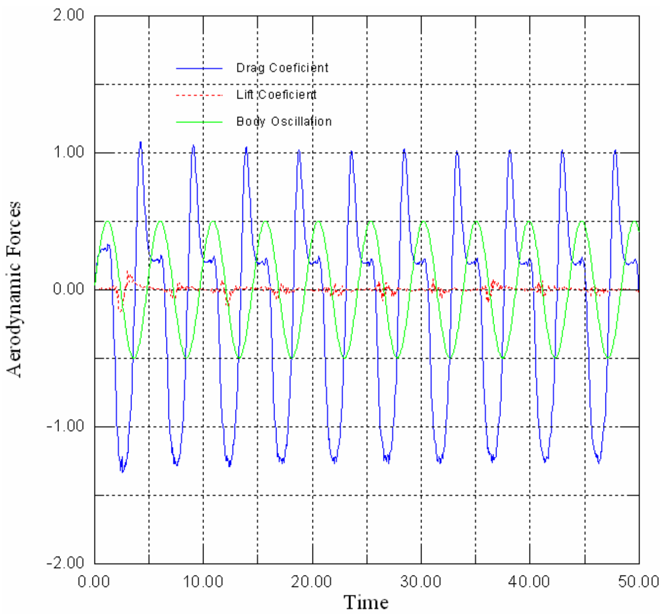

(b) $A_x/d=0.50$ and $f_{bx}/f_{cd}=1.0$

Figure 4. Time history of drag and lift coefficients for in-line oscillating cylinder.

For the symmetrical mode, a pair of vortices is shed in phase from both sides of the cylinder during one oscillation cycle.

Figure 5 illustrates the symmetrical mode of vortex formation; see Fig. 4b, where a pair of vortices is shed in phase from both sides of the cylinder during one oscillation cycle. The present numerical simulation runs ended with 80,000 discrete vortices. The final CPU time was about 10h when using a Intel(R) Core(TM)2 Quad CPU, without parallel computation.

Because the distributed vorticity of the mainstream flow has been replaced in the numerical model by a cloud of vortex particles, the CPU time for vortex-vortex interaction turns expensive. No attempts to simulate the flow for NP greater than 100 were made since the operation count of present algorithm is proportional to the square of Z.

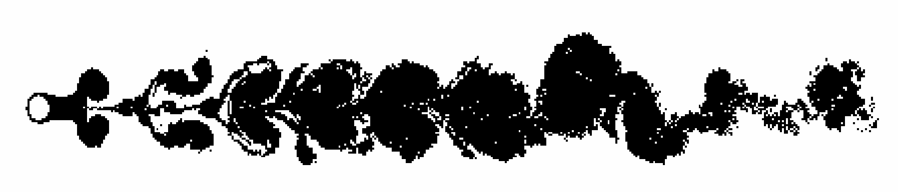

Figure 5. Symmetrical mode of vortex formation for in-line circular cylinder vibration ($A_x/d=0.5$ and $f_{bx}/f_{cd}=1.0$).

Further analyses will be carried out to understand the aerodynamic loads and vortex shedding behavior through different oscillating frequencies and amplitudes.

5. CONCLUSIONS

Drag and lift coefficients are computed to describe different flow regimes and their relations to the vortex shedding and to the harmonic motions of the circular cylinder. The methodology proposed permits to obtain results that have good agreement with the experimental results and it is greatly simplified by the utilization of the vortex method.

The forced body oscillation motions reveal different regimes of vortex shedding when the forcing frequency is close to the free vortex shedding frequency for both in-line and transversal motions of the cylinder in a fluid at rest. The vortex formation seems to be a predominant function of the oscillation amplitude and frequency than the Reynolds number.

Even for large Reynolds number, two-dimensional flow assumption is adopted at the present work, which is expected to show the main features of the vortex shedding phenomenon and predict this fluid-structure interaction problem in a qualitatively sense. Despite the differences presented, the results are promising, that encourages performing additional tests in order to explore the phenomena in more details.

In order to handle fluid flow and heat transfer by vortex method, a new method will be carried out (Recicar *et al.*, 2008).

6. ACKNOWLEDGEMENTS

This research was supported by the CNPq (Brazilian Research Agency) Proc. 470420/2008-1, FAPERJ (Research Foundation of the State of Rio de Janeiro) Proc. E-26/112/013/2008 and FAPEMIG (Research Foundation of the State of Minas Gerais) Proc. TEC APQ-01074-08.

7. REFERENCES

Alcântara Pereira, L.A., Hirata, M.H. and Manzanares Filho, N., 2004, "Wake and Aerodynamics Loads in Multiple Bodies - Application to Turbomachinery Blade Rows", J. Wind Eng. Ind. Aerodyn., 92, pp. 477-491.

Alcântara Pereira, L.A., Ricci, J.E.R., Hirata, M.H. and Silveira-Neto, A., 2002, "Simulation of Vortex-Shedding Flow about a Circular Cylinder with Turbulence Modeling", Intern'l Society of CFD, Vol. 11, No. 3, October, pp. 315-322.

Bearman, P.W., 1984, "Vortex Shedding from Oscillating Bluff Bodies", Annu. Rev. Fluid Mech., 16:195-222.

Blevins, R.D., 1990, "Flow Induced Vibrations", New York, Van Nostrand Reinhold.

Blevins, R. D., 1984, Applied Fluid Dynamics Handbook, Van Nostrand Reinhold, Co.

Chorin, A.J., 1973, "Numerical Study of Slightly Viscous Flow", Journal of Fluid Mechanics, Vol. 57, pp. 785-796.

Griffin, O.M. and Hall, M.S., 1991, "Review-Vortex Shedding Lock-On and Flow Control in Bluff Body Wakes", Journal of Fluids Engineering, Vol. 113, pp. 526-537.

Hirata, M. H., Alcântara Pereira, L. A., Recicar, J. N., Moura, W. H., 2008, "High Reynolds Number Oscillations of a Circular Cylinder", J. of the Braz. Soc. Of Mech. Sci. & Eng., Vol. XXX, No. 4, pp. 300-308.

Kamemoto, K., 2009, "Perspective Characteristics of a Lagrangian Vortex Method in Application into Vortex Flows of Moving Boundary Problems", Workshop – From fast cars to slow flows over bluff bodies, 20-30 June, Imperial College, London, UK.

Kamemoto, K., 1993, "Procedure to Estimate Unstead Pressure Distribution for Vortex Method" (In Japanese), Trans. Jpn. Soc. Mech. Eng., Vol. 59, No. 568 B, pp. 3708-3713.

Katz, J. and Plotkin, A., 1991, "Low Speed Aerodynamics: From Wing Theory to Panel Methods". McGraw Hill, Inc.

Koopman, G.H., 1967, "The Vortex Wakes of Vibrating Cylinders at Low Reynolds Numbers", Journal of Fluid Mechanics, Vol. 28, pp. 501-518.

Leonard, A., 1980, "Vortex Methods for Flow Simulation", J. Comput. Phys., Vol. 37, pp. 289-335.

Lewis, R.I., 1999, "Vortex Element Methods, the Most Natural Approach to Flow Simulation - A Review of Methodology with Applications", Proceedings of 1st Int. Conference on Vortex Methods, Kobe, Nov. 4-5, pp. 1-15.

Liu, S. and Song, F.U., 2003, "Regimes of Vortex Shedding from an In-Line Oscillating Circular Cylinder in the Uniform Flow", ACTA MECHANICA SINICA, Vol. 19, 2: 118-126.

Ongoren, A. and Rockwell, D., 1988, "Flow Structure from an Oscillating Cylinder. Part 2: Mode competition in the near Wake", Journal of Fluid Mechanics, 191: 225-245.

Recicar, J.N., Alcântara Pereira, L.A. and Hirata, M.H., 2008, "Fluid Flow AND Heat Transfer around na Oscillating Circular Cylinder Using a Particle Method", 12th Brazilian Congress of Thermal Engineering and Sciences, November 10-14, Belo Horizonte, MG.

Ricci, J.E.R., 2002, "Numerical Simulation of the Flow around a Body in the Vicinity of a Plane Using Vortex Method", Ph.D. Thesis, Mechanical Engineering Institute, UNIFEI, Itajubá, MG, Brazil (in Portuguese).

Sarpkaya, T., 1989, "Computational Methods with Vortices - The 1988 Freeman Scholar Lecture", Journal of Fluids Engineering, Vol. 111, pp. 5-52.

Sarpkaya, T., 1979, "Vortex-Induced Oscillations", ASME J. Appl. Mech., 46:241-258.

Shintani, M. and Akamatsu, T, 1994, "Investigation of Two Dimensional Discrete Vortex Method with Viscous Diffusion Model", Computational Fluid Dynamics Journal, Vol. 3, No. 2, pp. 237-254.

Stock, M.J., 2007, "Summary of Vortex Methods Literature (A lifting document rife with opinion)", April, 18: © 2002-2007 Mark J. Stock.

Uhlman, J.S., 1992, "An Integral Equation Formulation of the Equation of an Incompressible Fluid", Naval Undersea Warfare Center, T.R. 10-086.

Williamson, C.H.K. and Govardhan, R., 2004, "Vortex Induced Vibrations", Annu. Rev. Fluid Mech., 36:413-455.

Williamson, C.H.K. and Roshko, A., 1988, "Vortex Formation in the Wake of an Oscillating Cylinder", J. Fluids Struc, 2:355-81.

8. RESPONSIBILITY NOTICE

The author(s) is (are) the only responsible for the printed material included in this paper.